

# Influence of the distribution shape of porosity on the bending FGM new plate model resting on elastic foundations

Bekki Hadj<sup>\*1,2</sup>, Benferhat Rabia<sup>1,2</sup> and Tahar Hassaine Daouadji<sup>1,2</sup>

<sup>1</sup>Département de génie civil, Université Ibn Khaldoun Tiaret; BP 78 Zaaroura, Tiaret, Algérie.

<sup>2</sup>Laboratoire de Géomatique et Développement Durable, Université de Tiaret, Algérie.

(Received Decemver31, 2018, Revised April 6, 2019, Accepted May 10, 2019)

**Abstract.** The functionally graded materials (FGM) used in plates contain probably a porosity volume fraction which needs taking into account this aspect of imperfection in the mechanical behavior of such structures. The present work aims to study the effect of the distribution forms of porosity on the bending of simply supported FG plate reposed on the Winkler-Pasternak foundation. A refined theory of shear deformation is developed to study the effect of the distribution shape of porosity on static behavior of FG plates. It was found that the distribution form of porosity significantly influence the mechanical behavior of FG plates, in terms of deflection, normal and shear stress. It can be concluded that the proposed theory is simple and precise for the resolution of the behavior of flexural FGM plates resting on elastic foundations while taking into account the shape of distribution of the porosity.

**Keywords:** Functionally graded material; Higher-order theory; Volume fraction of porosity; Winkler–Pasternak elastic foundation, Navier’s solution

## 1. Introduction

Functionally graded materials (FGM) are, macroscopically, non-homogeneous compounds that are usually made from a mixture of metals and ceramics. FGM are considered as the most promising composite materials in various technology sectors such as aerospace, automotive, and defense industries, and recently electronics and biomedical industries.

In addition, the increasing use of plates as structural components in various fields such as marine technology; civil and aerospace has made it necessary to study their mechanical behavior. Several studies have been undertaken on the mechanical behavior of FGM plates. Cheng and Batra (2000), Tounsi (2013), Adim (2018), Hassaine Daouadji (2016), Belabed (2018), Bellifa (2017), Zohra (2016), Abualnour (2018), Bouadi (2018), Benhenni (2018), Rabia (2018), Rabahi (2018), Bensatallah (2018), Abdelaziz (2017), Chadad (2017), Tahar (2016) Benachour (2011), Hassaine Daouadji (2013) and Zenkour (2006), have studied the bending of a simply supported polygonal plate with a property gradient given by a first order shear deformation theory (FSDT). Praveen and Reddy (1998) also analyzed the nonlinear static and dynamic response of property gradient ceramic-metal plates in a constant temperature field and subjected to dynamic side loads by the finite element method. Park et al (2006) presented the post-buckling and thermal vibration behavior of the property gradient FGM plate, the nonlinear finite element

equations are based on the theory of first-order shear deformation plates and the stress relationship -Von Karman’s nonlinear displacement is used to account for the large displacement of the plate. Shen (2002) studied the nonlinear bending response of FG plates subjected to transverse loads and in a thermal environment.

Moreover, the functionally graded materials (FGM) used in plates may contain a porosity volume fraction which is the result of the imperfection in their construction. Thus, it is important to take this aspect in the study of the mechanical behavior of this type of structures. Benferhat et al. (2016a, 2016b, 2016c) studied the effect of porosity on the bending and free vibration response of functionally graded plates resting on Winkler-Pasternak foundations by introducing in the mathematical formulation a volume fraction of porosity.

The objective of this work is to use a refined theory of shear deformation to study the effect of the distribution form of porosity on static behavior of FGM plates. The effect due to porosity is included using a modified mixture law covering the porosity phases proposed by Wattanasakulpong (2012), Zaoui (2019), Belkacem (2016), Zine (2018), Khalifa (2018), Abdelhak (2016), Attia (2018), Mantari (2012), Menasria (2017), El Haina (2017), Mokhtar (2018), Fourn (2018), Benchorra (2018), Tahar (2017), Bouhadra (2018), Adim (2016), Youcef (2018), Slimane (2018), Demirhan (2019) and Younsi (2018). The properties of the material of the FGM plate are supposed to vary according to a power law distribution of the volume fraction of the constituents. The equation of motion for FGM plates is obtained by the principle of virtual works. The effects of power index, pore volume fraction, geometry ratio, and thickness ratio on FGM plate deflection are also studied.

\*Corresponding author, Ph.D.  
E-mail: [abekkihadj@yahoo.fr](mailto:abekkihadj@yahoo.fr)

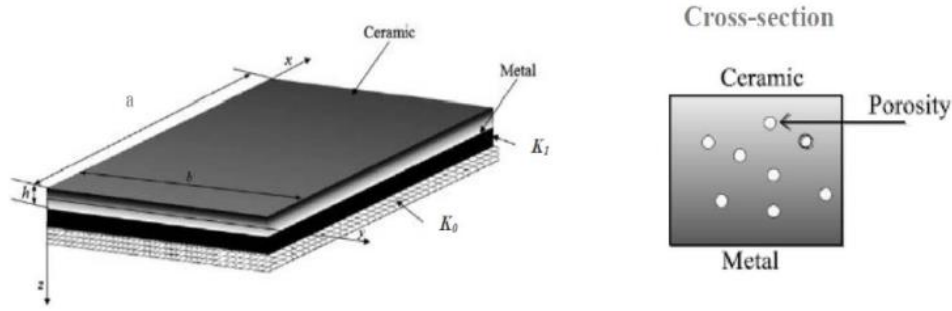


Fig. 1 Geometry and dimensions of the FGM plate resting on elastic foundation

Table 1 Deferent distribution forms of porosity

Distribution forms of Porosity	Elastic Modulus Expression	Schema
Homogeneous shape	$E = (e_c - e_m) \left( \frac{z}{h} + \frac{1}{2} \right)^k + e_m - (e_c + e_m) \frac{\alpha}{2}$	
Form "O" Shape	$E_2 = (e_c - e_m) * \left( \left( \frac{z}{t_2} + 0.5 \right)^k + e_m - (e_c + e_m) * \frac{\alpha}{2} * \left( 1 - 2 * \left  \frac{z}{t_2} \right  \right) \right)$	
Form "X" Shape	$E = (e_c - e_m) \left( \frac{z}{h} + \frac{1}{2} \right)^k + e_m - (e_c + e_m) \frac{\alpha}{2} \left( 2 \frac{z}{h} \right)$	
Form "V" Shape	$E = (e_c - e_m) \left( \frac{z}{h} + \frac{1}{2} \right)^k + e_m - (e_c + e_m) \frac{\alpha}{2} \left( \frac{1}{2} + \frac{z}{h} \right)$	

## 2. Geometric configuration and material properties

Consider an FGM plate of length  $a$ , width  $b$  and total thickness  $h$ , made of mixture of metal and ceramics, in which the composition is varied from the top to the bottom surface. The material in top surface and in bottom surface is ceramic and metal respectively (Fig. 1).

In this study, we consider an imperfect FGM plate with a volume fraction of porosity  $\alpha$  ( $\alpha \ll 1$ ), with different form of distribution between the metal and the ceramic. The modified mixture rule proposed by Wattanasakulpong (2014) and Benferhat (2014) is

$$P = P_m \left( V_m - \frac{\alpha}{2} \right) + P_c \left( V_c - \frac{\alpha}{2} \right) \quad (1)$$

The puissance law of the volume fraction of the ceramic is assumed as

$$V_c = \left( \frac{z}{h} + \frac{1}{2} \right)^k \quad (2)$$

The modified mixture rule becomes

$$P = (P_c - P_m) \left( \frac{z}{h} + \frac{1}{2} \right)^k + P_m - (P_c + P_m) \frac{\alpha}{2} \quad (3)$$

Where,  $k$  is the power law index that takes values greater than or equals to zero. The FGM plate becomes a fully ceramic plate when  $k$  is set to zero and fully metal for large value of  $k$ .

The Young's modulus ( $E$ ) of the imperfect FG can be written as a functions of thickness coordinate,  $Z$  (middle surface), as follows (Benferhat 2016b, Hassaine Daouadji 2016, Ait Athmane 2015, Ait Yahia 2015, Hadji 2015a, 2015b).

$$E(z) = (E_c - E_m) \left( \frac{z}{h} + \frac{1}{2} \right)^k + E_m - (E_c + E_m) \frac{\alpha}{2} \quad (4)$$

The material properties of a perfect FGM plate can be obtained when the volume fraction of porosity  $\alpha$  is set to zero. Due to the small variations of the Poisson ratio  $\nu$ , it is assumed to be constant. Several forms of porosity have been studied in the present work, such as "O", "V" and "X" (Table 1).

## 3. Displacement field and strains

Based on of the theory of the higher order shear deformation plate, displacement elements are assumed as follow

$$\begin{aligned} u(x, y, z_{ns}) &= u_0(x, y) - z \left[ 1 + \frac{3\pi}{2} \sec h^2 \left( \frac{1}{2} \right) \right] - \frac{3\pi}{2} h \tanh \left( \frac{z}{h} \right) \frac{\partial w_s}{\partial x} \\ v(x, y, z_{ns}) &= v_0(x, y) - z \left[ 1 + \frac{3\pi}{2} \sec h^2 \left( \frac{1}{2} \right) \right] - \frac{3\pi}{2} h \tanh \left( \frac{z}{h} \right) \frac{\partial w_s}{\partial y} \\ w(x, y, z_{ns}) &= w_b(x, y) + w_s(x, y) \end{aligned} \quad (5)$$

Linear deformation can be obtained from kinematic relationships as

$$\begin{aligned}
\varepsilon_x &= \varepsilon_x^0 + z k_x^b + z \left[ 1 + \frac{3\pi}{2} \sec^2 \left( \frac{1}{2} \right) \right] - \frac{3\pi}{2} h \tanh \left( \frac{z}{h} \right) k_x^s \\
\varepsilon_y &= \varepsilon_y^0 + z k_y^b + z \left[ 1 + \frac{3\pi}{2} \sec^2 \left( \frac{1}{2} \right) \right] - \frac{3\pi}{2} h \tanh \left( \frac{z}{h} \right) k_y^s \\
\gamma_{xy} &= \gamma_{xy}^0 + z k_{xy}^b + z \left[ 1 + \frac{3\pi}{2} \sec^2 \left( \frac{1}{2} \right) \right] - \frac{3\pi}{2} h \tanh \left( \frac{z}{h} \right) k_{xy}^s \\
\gamma_{yz} &= 1 - \frac{d \left( z \left[ 1 + \frac{3\pi}{2} \sec^2 \left( \frac{1}{2} \right) \right] - \frac{3\pi}{2} h \tanh \left( \frac{z}{h} \right) \right)}{dz} \gamma_{yz}^s \\
\gamma_{xz} &= 1 - \frac{d \left( z \left[ 1 + \frac{3\pi}{2} \sec^2 \left( \frac{1}{2} \right) \right] - \frac{3\pi}{2} h \tanh \left( \frac{z}{h} \right) \right)}{dz} \gamma_{xz}^s \\
\varepsilon_z &= 0
\end{aligned} \quad (6)$$

Where

$$\begin{aligned}
\varepsilon_x^0 &= \frac{\partial u_0}{\partial x}, \quad k_x^b = -\frac{\partial^2 w_b}{\partial x^2}, \quad k_x^s = -\frac{\partial^2 w_s}{\partial x^2} \\
\varepsilon_y^0 &= \frac{\partial v_0}{\partial y}, \quad k_y^b = -\frac{\partial^2 w_b}{\partial y^2}, \quad k_y^s = -\frac{\partial^2 w_s}{\partial y^2} \\
\gamma_{xy}^0 &= \frac{\partial u_0}{\partial y} + \frac{\partial v_0}{\partial x}, \quad k_{xy}^b = -2 \frac{\partial^2 w_b}{\partial x \partial y}, \quad k_{xy}^s = -2 \frac{\partial^2 w_s}{\partial x \partial y} \\
\gamma_{yz}^s &= \frac{\partial w_s}{\partial y}, \quad \gamma_{xz}^s = \frac{\partial w_s}{\partial x}, \quad g(z) = 1 - \frac{f(z)}{dz} \\
f(z) &= z \left[ 1 + \frac{3\pi}{2} \sec^2 \left( \frac{1}{2} \right) \right] - \frac{3\pi}{2} h \tanh \left( \frac{z}{h} \right)
\end{aligned} \quad (7)$$

The linear constitutive relationships of a FG plate can be written as

$$\begin{Bmatrix} \sigma_x \\ \sigma_y \\ \tau_{xy} \end{Bmatrix} = \begin{bmatrix} \frac{E(z)}{1-\nu^2} & \frac{\nu E(z)}{1-\nu^2} & 0 \\ \frac{\nu E(z)}{1-\nu^2} & \frac{E(z)}{1-\nu^2} & 0 \\ 0 & 0 & \frac{E(z)}{2(1+\nu)} \end{bmatrix} \begin{Bmatrix} \varepsilon_x \\ \varepsilon_y \\ \gamma_{xy} \end{Bmatrix} \quad (8)$$

$$\begin{Bmatrix} \tau_{yz} \\ \tau_{zx} \end{Bmatrix} = \begin{bmatrix} \frac{E(z)}{2(1+\nu)} & 0 \\ 0 & \frac{E(z)}{2(1+\nu)} \end{bmatrix} \begin{Bmatrix} \gamma_{yz} \\ \gamma_{zx} \end{Bmatrix} \quad (9)$$

#### 4. Equilibrium equations

The equilibrium equations that govern can be derived using the principle of virtual displacements. The principle of virtual work in this case gives

$$\int_{-h/2}^{h/2} \int_{\Omega} (\sigma_x \delta \varepsilon_x + \sigma_y \delta \varepsilon_y + \tau_{xy} \delta \gamma_{xy} + \tau_{yz} \delta \gamma_{yz} + \tau_{zx} \delta \gamma_{zx}) d\Omega dz + \int_{\Omega} [f_c \delta w] d\Omega - \int_{\Omega} [q \delta w] d\Omega = 0 \quad (10)$$

Where  $\Omega$  is the upper surface,  $f_c$  is the density of the foundation reaction force.

For the Pasternak foundation model,  $f_c$  can be written as

$$f_c = K_0 w - K_1 \nabla^2 w \quad (11)$$

$K_0$  and  $K_1$  are the transverse and shear stiffness coefficients of the foundation respectively.

The stress resultants are given as

$$\begin{Bmatrix} N \\ M^b \\ M^s \end{Bmatrix} = \begin{bmatrix} A & B & B^s \\ A & D & D^s \\ B^s & D^s & H^s \end{bmatrix} \begin{Bmatrix} \varepsilon \\ k^b \\ k^s \end{Bmatrix}, \quad S = A^s \gamma \quad (12)$$

Where

$$N = \{N_x, N_y, N_{xy}\}^T, \quad M^b = \{M_x^b, M_y^b, M_{xy}^b\}^T, \quad (13)$$

$$\begin{aligned}
M^s &= \{M_x^s, M_y^s, M_{xy}^s\}^T, \quad \varepsilon = \{\varepsilon_x^0, \varepsilon_y^0, \varepsilon_{xy}^0\}^T, \\
k^b &= \{k_x^b, k_y^b, k_{xy}^b\}^T, \quad k^s = \{k_x^s, k_y^s, k_{xy}^s\}^T \\
A &= \begin{bmatrix} A_{11} & A_{12} & 0 \\ A_{12} & A_{22} & 0 \\ 0 & 0 & A_{66} \end{bmatrix}, \quad B = \begin{bmatrix} B_{11} & B_{12} & 0 \\ B_{12} & B_{22} & 0 \\ 0 & 0 & B_{66} \end{bmatrix}, \quad D = \begin{bmatrix} D_{11} & D_{12} & 0 \\ D_{12} & D_{22} & 0 \\ 0 & 0 & D_{66} \end{bmatrix} \\
B^s &= \begin{bmatrix} B_{11}^s & B_{12}^s & 0 \\ B_{12}^s & B_{22}^s & 0 \\ 0 & 0 & B_{66}^s \end{bmatrix}, \quad D^s = \begin{bmatrix} D_{11}^s & D_{12}^s & 0 \\ D_{12}^s & D_{22}^s & 0 \\ 0 & 0 & D_{66}^s \end{bmatrix}, \quad H^s = \begin{bmatrix} H_{11}^s & H_{12}^s & 0 \\ H_{12}^s & H_{22}^s & 0 \\ 0 & 0 & H_{66}^s \end{bmatrix} \\
S &= \{S_{xz}^s, S_{yz}^s\}^T, \quad \gamma = \{\gamma_{xz}^s, \gamma_{yz}^s\}^T, \quad A^s = \begin{bmatrix} A_{44}^s & 0 \\ 0 & A_{55}^s \end{bmatrix}
\end{aligned}$$

Stiffness components and inertias are given as

$$\begin{aligned}
&\{A_{ij}, B_{ij}, C_{ij}, D_{ij}, E_{ij}, G_{ij}\} \\
&= \int_{-h/2}^{h/2} \{1, z_{ns}, f(z_{ns}), z_{ns}^2, z_{ns} f(z_{ns}), [f(z_{ns})]^2\} Q_{ij} dz_{ns} \quad (14)
\end{aligned}$$

Following the Navier solution procedure, we assume that the following solution form  $u_0$ ,  $v_0$ ,  $w_b$  and  $w_s$ , satisfies the boundary conditions

$$\begin{Bmatrix} u_0 \\ v_0 \\ w_b \\ w_s \end{Bmatrix} = \sum_{m=1}^{\infty} \sum_{n=1}^{\infty} \begin{Bmatrix} U_{mn} \cos(\lambda x) \sin(\mu y) \\ V_{mn} \sin(\lambda x) \cos(\mu y) \\ W_{bmn} \sin(\lambda x) \sin(\mu y) \\ W_{smn} \sin(\lambda x) \sin(\mu y) \end{Bmatrix} \quad (15)$$

Where:  $\lambda = m\pi/a$ ,  $\mu = n\pi/b$  et  $U_{mn}$ ,  $V_{mn}$ ,  $W_{bmn}$ ,  $W_{smn}$  are arbitrary parameters to be determined. We obtain the equation of the following operator

$$([K]\{\Delta\} = \{F\}) \quad (16)$$

Where  $\{\Delta\} = \{U, V, W_b, W_s\}^T$ .  $[K]$  is the stiffness matrices, represented as

$$[K] = \begin{bmatrix} a_{11} & a_{12} & a_{13} & a_{14} \\ a_{12} & a_{22} & a_{23} & a_{24} \\ a_{13} & a_{23} & a_{33} & a_{34} \\ a_{14} & a_{24} & a_{34} & a_{44} \end{bmatrix} \quad (17)$$

In which

$$\begin{aligned}
a_{11} &= A_{11}\alpha^2 + A_{66}\beta^2, a_{12} = \alpha\beta(A_{12} + A_{66}), a_{13} = -B_{11}\alpha^3 \\
a_{14} &= C_{11}\alpha^2 + C_{66}\beta^2, a_{15} = \alpha\beta(C_{12} + C_{66}), a_{22} = A_{66}\alpha^2 + A_{22}\beta^2 \\
a_{23} &= -B_{22}\beta^3, a_{24} = \alpha\beta(C_{12} + C_{66}), a_{25} = C_{66}\alpha^2 + C_{22}\beta^2 \\
a_{33} &= D_{11}\alpha^4 + 2D_{12}\alpha^2\beta^2 + 4D_{66}\alpha^2\beta^2 + D_{22}\beta^4 + k_0 + k_1(\alpha^2 + \beta^2) \\
a_{34} &= -E_{11}\alpha^3 - E_{12}\alpha\beta^2 - 2E_{66}\alpha\beta^2, a_{45} = \alpha\beta(G_{12} + G_{66}) \\
a_{35} &= -E_{12}\alpha^2\beta - 2E_{66}\alpha^2\beta - E_{22}\beta^3, a_{44} = F_{55} + G_{11}\alpha^2 + G_{66}\beta^2 \\
a_{55} &= F_{44} + G_{66}\alpha^2 + G_{22}\beta^2
\end{aligned} \quad (18)$$

#### 5. Results and discussion

In this study, flexural analysis of fgm plates by the new hyperbolic theory of shear deformation of the plate is suggested for investigation, the effect of the distribution form of porosity is also studied; the Poisson's ratio is fixed at  $\nu=0.3$ . Comparisons are made with the solutions available in the literature in order to verify the accuracy of this analysis. The properties of the materials used in this analysis are presented in table 2.

Table 2 Materials proprieties

Materiel	Properties	
	E (GPa)	$\nu$
Ceramic (Alumina, $\text{Al}_2\text{O}_3$ )	380	0.3
Ceramic (Zirconia, $\text{ZrO}_2$ )	151	0.3
Metal (Aluminum Al)	70	0.3

Table 3 Maximum dimensionless deflections of fgm plates without elastic foundations under uniform loads

Theory	$\alpha$	a = b			a = 0.5b		
		a/h = 25	10	5	a/h = 25	10	5
Reddy (2001)	$\alpha = 0$	0.410	0.427	0.490	1.018	1.045	1.043
Cooke (1883)	$\alpha = 0$	0.410	0.427	0.490	1.018	1.045	1.043
Lee (2002)	$\alpha = 0$	0.410	0.427	0.490	1.018	1.045	1.043
Zenkour (2018)	$\alpha = 0$	0.410	0.427	0.490	1.018	1.045	1.043
Present	$\alpha = 0$	0.40960	0.42725	0.49019	1.01806	1.04536	1.14273
	$\alpha = 0.1$	0.43537	0.454148	0.52104	1.08214	1.11115	1.21465
	$\alpha = 0.2$	0.46462	0.484650	0.55603	1.154823	1.18578	1.29623

Table 4 Effects of side-to-thickness ration on the deflections 10W of homogeneous square plate resting on elastic foundations under uniform loads for thickness ratio a/h=5.

$K_0$	$K_1$	Carrera (2011)	Thai (2013)	Zenkour (2018)	Present theory		
		$\alpha = 0$	$\alpha = 0$	$\alpha = 0$	$\alpha = 0$	$\alpha = 0.1$	$\alpha = 0.2$
1	5	3.7069	3.7061	3.7058	3.70571	3.87910	4.06947
	10	2.9810	2.9806	2.9805	2.98040	3.09117	3.21042
	15	2.4906	2.4904	2.4903	2.49026	2.56680	2.64812
	20	2.1375	2.1373	2.1373	2.13727	2.19315	2.25195
34	5	3.0859	3.0855	3.0853	3.08527	3.20390	3.33191
	10	2.5623	2.5621	2.5620	2.56202	2.64288	2.72889
	15	2.1893	2.1892	2.1892	2.18918	2.24763	2.30918
	20	1.9104	1.9103	1.9103	1.91028	1.95440	2.00051
54	5	1.4029	1.4032	1.4032	1.40325	1.42445	1.44595
	10	1.2809	1.2811	1.2811	1.28116	1.29877	1.31662
	15	1.1784	1.1785	1.1786	1.17861	1.19349	1.20854
	20	1.0911	1.0912	1.0912	1.09127	1.10400	1.11687

Table 5 Effects of side-to-thickness ration on the deflections 10W of homogeneous square plate resting on elastic foundations under uniform loads for thickness ratio a/h=10

$K_0$	$K_1$	Perfect plate $\alpha = 0$				Imperfect plate $\alpha = 0.1$	Imperfect plate $\alpha = 0.2$
		Carrera (2011)	Thai (2013)	Zenkour (2018)	Present	Present	Present
1	5	3.3455	3.3455	3.3454	3.34539	3.50783	3.68684
	10	2.7505	2.7504	2.7504	2.75039	2.85894	3.25018
	15	2.3331	2.3331	2.3330	2.33303	2.41036	2.49292
	20	2.0244	2.0244	2.0244	2.02436	2.08205	2.14305
34	5	2.8422	2.8421	2.8421	2.84207	2.95805	3.08383
	10	2.3983	2.3983	2.3983	2.39827	2.47997	2.56734
	15	2.0730	2.0730	2.0730	2.07295	2.13339	2.19737
	20	1.8245	1.8244	1.8244	1.82444	1.87083	1.91954
54	5	1.3785	1.3785	1.3785	1.37847	1.40308	1.42832
	10	1.2615	1.2615	1.2615	1.26151	1.28192	1.30276
	15	1.1627	1.1627	1.1627	1.16273	1.17991	1.19740
	20	1.0782	1.0782	1.0782	1.07822	1.09286	1.10774

The dimensionless deflections of simply supported fgm plates under uniformly distributed loading, for different values of thickness ratio a/h, are presented in table 3. The calculated dimensionless deflections are compared with those reported in literature (Reddy 2001; Cooke and Levinson, 1983; Lee 2002, Zenkour and Radwan, 2018).

As we can see on table 3, close agreements were obtained between the results of the present method and those of literature (when  $\alpha = 0$ ; perfect plate). It can be noted that deflections increases by increasing the thickness ratio a/h. By introducing the volume fraction of porosity ( $\alpha$ ), it can be noted that the increase of this factor induces an

Table 6 Effects of side-to-thickness ratio on the deflections 10W of homogeneous square plate resting on elastic foundations under uniform loads for thickness ratio  $a/h=100$ 

$K_0$	$K_1$	Perfect plate $\alpha=0$				Imperfect plate $\alpha=0.1$	Imperfect plate $\alpha=0.2$
		Carrera (2011)	Thai (2013)	Zenkour (2018)	Present	Present	Present
1	5	3.2200	3.2200	3.2200	3.22099	3.37941	3.55419
	10	2.6684	2.6684	2.6684	2.66906	2.77665	2.89323
	15	2.2763	2.2763	2.2763	2.27674	2.35427	2.43720
	20	1.9834	1.9834	1.9834	1.98372	2.04206	2.10385
34	5	2.7552	2.7552	2.7552	2.75588	2.87070	2.99544
	10	2.3390	2.3390	2.3389	2.33940	2.42129	2.50904
	15	2.0306	2.0306	2.0306	2.03094	2.09207	2.15690
	20	1.7932	1.7932	1.7932	1.79343	1.84067	1.89036
54	5	1.3688	1.3688	1.3688	1.36886	1.39481	1.42152
	10	1.2543	1.2543	1.2543	1.25430	1.27585	1.29793
	15	1.1572	1.1572	1.1572	1.15727	1.175418	1.19395
	20	1.0740	1.0740	1.0740	1.07403	1.08951	1.10526

Table 7 Nondimensional deflections 10w of homogeneous plates resting on elastic foundations and subjected to uniformly distributed loads ( $K_0 = 10$  ;  $K_1 = 10$ )

a/b	a/h	Perfect plate $\alpha=0$			Imperfect plate $\alpha=0.1$	Imperfect plate $\alpha=0.2$
		Zenkour (2018)	Thai (2013)	Present	Present	Present
0.5	5	5.5718	5.5720	5.57180	5.73543	5.90875
	10	5.3562	5.3563	5.35625	5.52191	5.69793
	100	5.2811	5.2811	5.28105	5.44736	5.62427
1.0	5	2.9270	2.9271	2.92694	3.03363	3.14832
	10	2.7059	2.7059	2.70588	2.81083	2.92418
	100	2.6276	2.6276	2.62756	2.73172	2.84442
2.0	5	0.7165	0.7165	0.71627	0.74946	0.78588
	10	0.5736	0.5736	0.57362	0.60223	0.63384
	100	0.5219	0.5219	0.52188	0.54860	0.57821

Table 8 Nondimensional deflections 10w of homogeneous plates resting on elastic foundations and subjected to uniformly distributed loads ( $K_0 = 10$  ;  $K_1 = 100$ )

a/b	a/h	Perfect plate $\alpha=0$			Imperfect plate $\alpha=0.1$	Imperfect plate $\alpha=0.2$
		Zenkour (2018)	Thai (2013)	Present	Present	Present
0.5	5	1.0371	1.0371	1.03713	1.04227	1.04744
	10	1.0330	1.0330	1.03303	1.03847	1.04396
	100	1.0320	1.0320	1.03199	1.03755	1.04314
1.0	5	0.6451	0.6450	0.64507	0.64981	0.65460
	10	0.6383	0.6383	0.63827	0.64347	0.64873
	100	0.6364	0.6364	0.63639	0.64177	0.64721
2.0	5	0.2207	0.2207	0.22069	0.22368	0.22675
	10	0.2069	0.2069	0.20690	0.21040	0.21401
	100	0.2013	0.2012	0.20125	0.20498	0.20884

Table 9 Nondimensional deflections 10w of homogeneous plates resting on elastic foundations and subjected to uniformly distributed loads ( $K_0 = 100$  ;  $K_1 = 10$ )

a/b	a/h	Perfect plate $\alpha=0$			Imperfect plate $\alpha=0.1$	Imperfect plate $\alpha=0.2$
		Zenkour (2018)	Thai (2013)	Present	Present	Present
0.5	5	4.0769	4.0769	4.07690	4.16116	4.24863
	10	3.9791	3.9791	3.97907	4.06732	4.15922
	100	3.9447	3.9446	3.94464	4.03433	4.12785
1.0	5	2.4787	2.4788	2.47872	2.55417	2.63423
	10	2.3271	2.3271	2.32710	2.40383	2.48569
	100	2.2724	2.2724	2.27242	2.34951	2.43192
2.0	5	0.6844	0.6844	0.68423	0.71443	0.74740
	10	0.5536	0.5536	0.55362	0.58021	0.60947
	100	0.5056	0.5056	0.50560	0.53063	0.55826

Table 10 Nondimensional deflections 10w of homogeneous plates resting on elastic foundations and subjected to uniformly distributed loads ( $K_0 = 100$  ;  $K_1 = 100$ )

a/b	a/h	Perfect plate $\alpha=0$			Imperfect plate $\alpha=0.1$	Imperfect plate $\alpha=0.2$
		Zenkour (2018)	Thai (2013)	Present	Present	Present
0.5	5	0.9679	0.9679	0.96790	0.97230	0.97671
	10	0.9649	0.9649	0.96489	0.96954	0.97422
	100	0.9643	0.9642	0.96425	0.96899	0.97375
1.0	5	0.6190	0.6190	0.61899	0.62331	0.62768
	10	0.6132	0.6132	0.61318	0.61792	0.62272
	100	0.6117	0.6117	0.61168	0.61792	0.62272
2.0	5	0.2174	0.2174	0.21742	0.22032	0.22329
	10	0.2041	0.2041	0.20410	0.20750	0.21101
	100	0.1987	0.1987	0.19865	0.20228	0.20604

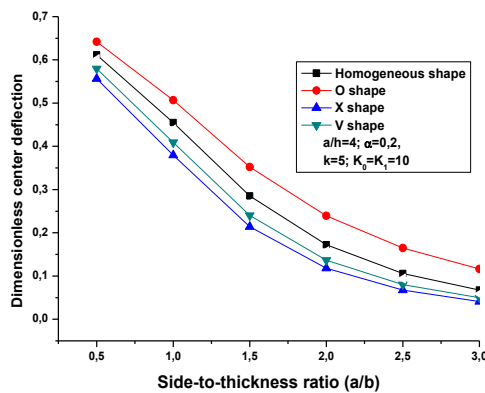


Fig. 2 Effect of the shape of porosity distribution on the dimensionless deflections versus aspect ratio  $a/b$  of an Al/Al<sub>2</sub>O<sub>3</sub> fgm plate resting on an elastic foundation ( $a/h=4$ ;  $\alpha=0.2$ )

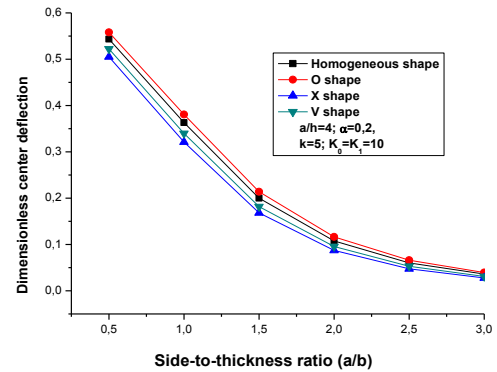


Fig. 3 Effect of the shape of porosity distribution on the dimensionless deflections versus aspect ratio  $a/b$  of an Al/ZrO<sub>2</sub> fgm plate resting on an elastic foundation ( $a/h=4$ ;  $\alpha=0.2$ )

increase in dimensionless deflections, which shows that the porosity has a significant influence on the deflections of fgm plates. In table 4, 5 and 6, we present the Effects of side-to-thickness ratio on the deflections 10w of homogeneous square plate resting on elastic foundations under uniform loads for deferent values of the thickness ratio  $a/h = 5, 10$  and  $100$  respectively. By comparing the deferent results presented in (tables) 4-6, It can be noted that the present method gives deflections values very closer to those obtained with other literature methods (Carrera 2011;Thai 2013, Zenkour 2018).

In tables 7-10, Nondimensional deflections 10w of homogeneous plates resting on elastic foundations and subjected to uniformly distributed loads, for deferent values of  $K_0$  and  $K_1$ , for deferent thickness ratio and side to thickness ratio are presented.

By analyzing the previous results presented in tables 7-10 and compared to those of literature, it can be noted that the present method is in good agreement with the others literature methods for deferent cases (thickness ratio, deferent values of  $K_0$  and  $K_1$  and side to thickness ratio. The results presented in previous tables reveal that the increase in volume fraction porosity increase the deflections of fgm plates which is consistent with the previous results.

In fig.2 and fig.3, we present the effect of the distribution shape of porosity on the dimensionless deflections of FG plate, resting on an elastic foundation for deferent aspect ratio  $a/b$ , made with Al/Al<sub>2</sub>O<sub>3</sub> and Al/ ZrO<sub>2</sub> respectively. As we can seen on fig.2 and fig. 3, the dimensionless deflections decrease in increasing the aspect ratio  $a/b$  (length to width).

It can also be noted that the distribution shape of porosity slightly influences the variation of the dimensionless deflections as a function of the geometry ratio. The highest values of dimensionless were obtained for the "O" shape of porosity distribution while the lowest ones correspond to the "V" shape of porosity distribution. Comparing the two fgm plates, it can be noted that the deferent curves are spaced for the plate made with Al/Al<sub>2</sub>O<sub>3</sub> than for that made with Al/ZrO<sub>2</sub>. It can also be observed that the deferent curves respect the same order for deferent distribution shape of porosity.

In fig.4 and fig.5, we present the effect of the distribution shape of porosity on the dimensionless deflections of fgm square plate, resting on an elastic foundation for deferent side to thickness ratio  $a/h$ , made with Al/Al<sub>2</sub>O<sub>3</sub> and Al/ZrO<sub>2</sub> respectively. It should be noted that the effect of the distribution shape of porosity on the dimensionless deflection is very significant by increasing thickness ratio (as the plate becomes thinner).



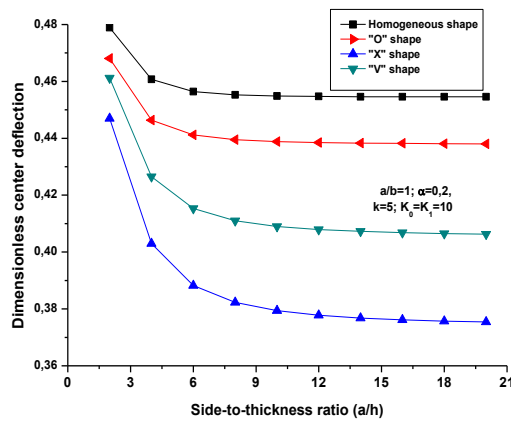


Fig. 4 Effect of the shape of porosity distribution on the dimensionless deflections versus side-to-thickness ratio  $a/h$  of an Al/Al<sub>2</sub>O<sub>3</sub> fgm square plate resting on an elastic foundation ( $a/b=1$ ;  $\alpha=0.2$ )

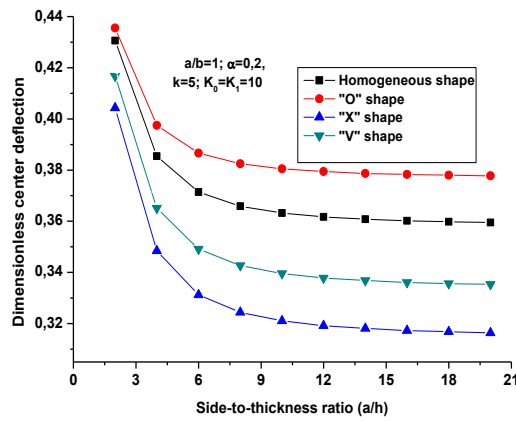


Fig. 5 Effect of the shape of porosity distribution on the dimensionless deflections versus side-to-thickness ratio  $a/h$  of an Al/ZrO<sub>2</sub> fgm square plate resting on an elastic foundation ( $a/b=1$ ;  $\alpha=0.2$ )

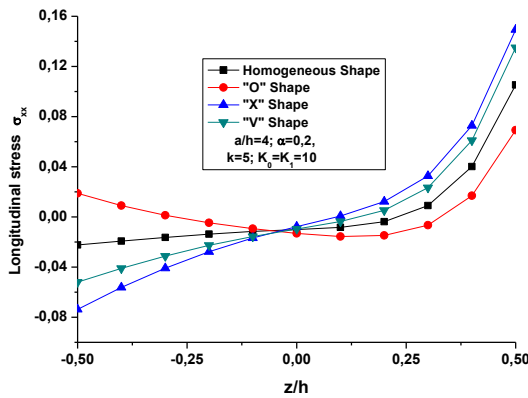


Fig. 6 Effect of the shape of porosity distribution on the longitudinal stress across the thickness of an Al/Al<sub>2</sub>O<sub>3</sub> fgm square plate resting on an elastic foundation ( $a/h=4$ ;  $\alpha=0.2$ )

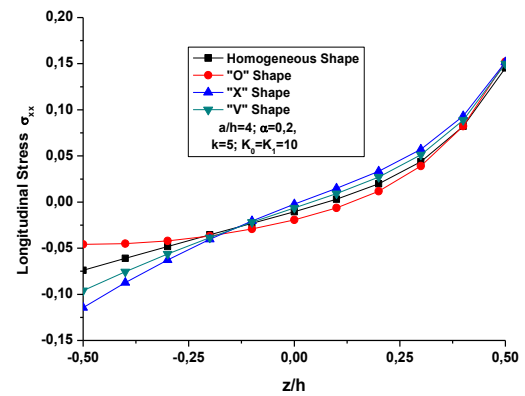


Fig. 7 Effect of the shape of porosity distribution on the longitudinal stress across the thickness of an Al/Al/ZrO<sub>2</sub> fgm square plate resting on an elastic foundation ( $a/h=4$ ;  $\alpha=0.2$ )

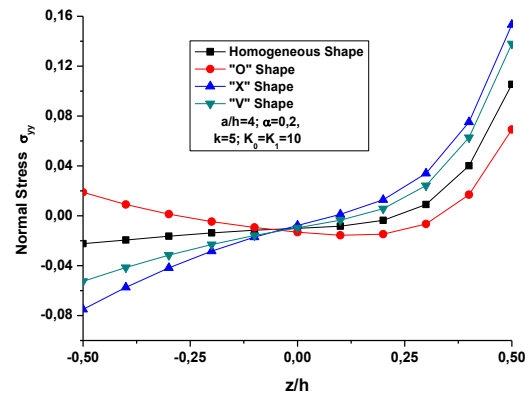


Fig. 8 Effect of the shape of porosity distribution on the Normal stress  $\sigma_{yy}$  across the thickness of an Al/Al<sub>2</sub>O<sub>3</sub> fgm square plate resting on an elastic foundation ( $a/h=4$ ;  $\alpha=0.2$ )

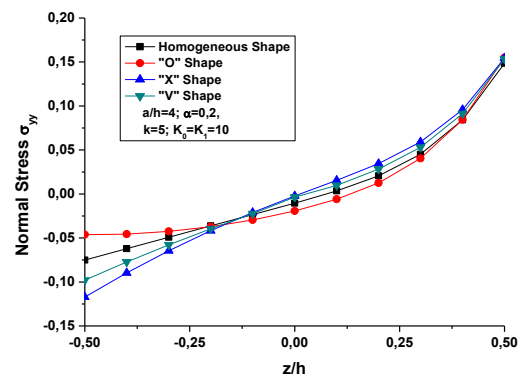


Fig. 9 Effect of the shape of porosity distribution on the Normal stress  $\sigma_{yy}$  across the thickness of an Al/ZrO<sub>2</sub> fgm square plate resting on an elastic foundation ( $a/h=4$ ;  $\alpha=0.2$ )

The effect of the distribution shape of porosity on the longitudinal stress across the thickness of an Al/Al<sub>2</sub>O<sub>3</sub> and Al/ZrO<sub>2</sub> fgm square plate resting on a Winkler-Pasternak type foundation is presented in fig.6 and fig.7, respectively.

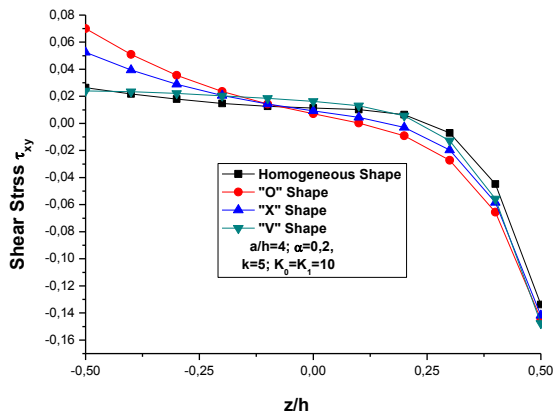


Fig. 10 Effect of the shape of porosity distribution on the shear stress  $\tau_{xy}$  across the thickness of an Al/Al<sub>2</sub>O<sub>3</sub> fgm square plate resting on an elastic foundation ( $a/h=4$ ;  $\alpha=0.2$ )

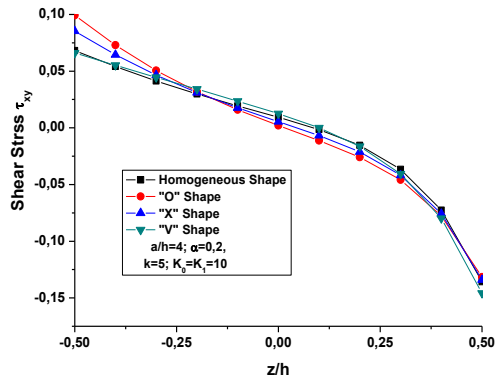


Fig. 11 Effect of the shape of porosity distribution on the shear stress  $\tau_{xy}$  across the thickness of an Al/ZrO<sub>2</sub> fgm square plate resting on an elastic foundation ( $a/h=4$ ;  $\alpha=0.2$ )

According to these figures, it is clear that the longitudinal stress is maximum for "X" distribution shape of porosity and it is minimal for "O" distribution shape of porosity. It can be noted particularly that the influence of the distribution shape of porosity is more significant for the Al/Al<sub>2</sub>O<sub>3</sub> fgm plate than for the Al/ZrO<sub>2</sub> FG plate.

The fig. 8 and fig.9 show the influence of distribution shape of porosity on the normal stress of an Al/Al<sub>2</sub>O<sub>3</sub> and Al/ZrO<sub>2</sub> fgm plate, respectively. The parameters of Winkler and Pasternak are taken equal to  $K_0=K_1=10$ . The volume fraction of porosity is taken equal to 0.2. The same tendency was observed for the influence of this parameter on the normal stress as on the longitudinal stress. As we can see on the fig. 10 and fig. 11, the shear stress decrease by increasing the thickness ratio  $a/h$  of an Al/Al<sub>2</sub>O<sub>3</sub> and Al/ZrO<sub>2</sub> FGM plate, respectively. It can be also noted that the distribution shape of porosity has an influence on the shear stress, particularly in the lower of the fgm plate (metal side).

## 5. Conclusions

The study was focused on the effect of the distribution shape of porosity on flexion fgm plates based on a two-parameter elastic foundation. The mathematical formulation is based on the use of the refined theory of shear deformation. The properties of the material are assumed to vary according to the thickness direction of the plate and the rule of the mixture that has been reformulated to evaluate the characteristics of the materials with different distribution shape of porosity. The Navier method is used for analytical solutions of the fgm plate with simply supported boundary conditions. A parametric study was conducted, including volume fraction indices, geometry ratios, thickness ratios, foundation stiffness parameters and volume fraction of porosity. According to the typical results, it can be concluded that distribution shape of porosity has a significant effect on the deflections of fgm plates as well as on the normal and shear stress developed in the plate. Finally, it is up to the researchers and manufacturer to choose wisely the material combinations that gives rise to a fgm plate offers rigidity, strength and most of all less greedy in terms of cost. In view of this research, it is very important to study the effect of boundary conditions, and to see how these boundary conditions can affect the stability of this type of porous plate.

## Acknowledgments

This research was supported by the French Ministry of Foreign Affairs and International Development (MAEDI) and Ministry of National Education, Higher Education and Research (MENESR) and by the Algerian Ministry of Higher Education and Scientific Research (MESRS) under Grant No. PHC Tassili 17MDU992. Their support is greatly appreciated.

## References

- Abdelaziz, H. H., Meziane, M. A. A., Bousahla, A. A., Tounsi, A., Mahmoud, S. R. and Alwabli, A. S. (2017), "An efficient hyperbolic shear deformation theory for bending, buckling and free vibration of FGM sandwich plates with various boundary conditions", *Steel Compos. Struct.*, **25**(6), 693-704. <https://doi.org/10.12989/scs.2017.25.6.693>.
- Abdelbasset, C., Hassaine Daouadji, T., Abderezak, R., Belkacem, A., Abbes, B., Rabia, B. and Abbes, F. (2017), "A high-order closed-form solution for interfacial stresses in externally sandwich FGM plated RC beams", *Adv. Mater. Res.*, **6**(4), 317-328. <https://doi.org/10.12989/amr.2017.6.4.317>.
- Abdelhak Z., Lazreg Hadji, Z. Khelifa, T. Hassaine daouadji and E.A. Adda Bedia, (2016) "Analysis of buckling response of functionally graded sandwich plates using a refined shear deformation theory", *Wind Struct.*, **22**(3), 291-305. <https://doi.org/10.12989/was.2016.22.3.291>.
- Abualnour, M., Houari, M. S. A., Tounsi, A. and Mahmoud, S. R. (2018), "A novel quasi-3D trigonometric plate theory for free vibration analysis of advanced composite plates", *Compos. Struct.*, **184**, 688-697.
- Adim B., T. Hassaine Daouadji, B. Abbas, A. Rabahi (2016) "Buckling and free vibration analysis of laminated composite



- plates using an efficient and simple higher order shear deformation theory", *J. Mech. Industry*, **17**(5), 512. <https://doi.org/10.1051/meca/2015112>.
- Ait Atmane, H., Tounsi, A. and Bernard, F. (2015), "Effect of thickness stretching and porosity on mechanical response of a functionally graded beams resting on elastic foundations", *Int. J. Mech. Mater.*, 1-14. <https://doi.org/10.1007/s10999-015-9318-x>.
- Ait Yahia, S., Ait Atmane, H., Houari, M.S.A. and Tounsi, A. (2015), "Wave propagation in functionally graded plates with porosities using various higher-order shear deformation plate theories", *Struct. Eng. Mech.*, **53**(6), 1143-1165. <http://dx.doi.org/10.12989/sem.2015.53.6.1143>.
- Attia, A., Bousahla, A. A., Tounsi, A., Mahmoud, S. R. and Alwabli, A. S. (2018), "A refined four variable plate theory for thermoelastic analysis of FGM plates resting on variable elastic foundations", *Struct. Eng. Mech.*, **65**(4), 453-464. <https://doi.org/10.12989/sem.2018.65.4.453>.
- Belabed, Z., Bousahla, A. A., Houari, M. S. A., Tounsi, A. and Mahmoud, S. R (2018), "A new 3-unknown hyperbolic shear deformation theory for vibration of functionally graded sandwich plate", *Earthq. Struct.*, **14**(2), 103-115. <https://doi.org/10.12989/eas.2018.14.2.103>.
- Belkacem, A., Hassaine Daouadji, T., Rabia, B. and Hadji, L. (2016), "An efficient and simple higher order shear deformation theory for bending analysis of composite plates under various boundary conditions", *Earthq. Struct.*, **11**(1), 63-82.
- Belkacem, A., Tahar Hassaine Daouadji, Rabahi Abderrezak, Benhenni Mohamed Amine, Zidour Mohamed and Abbes Boussad (2018), "Mechanical buckling analysis of hybrid laminated composite plates under different boundary conditions", *Struct. Eng. Mech.*, **66**(6), 761-769. <https://doi.org/10.12989/sem.2018.66.6.761>.
- Bellifa, H., Bakora, A., Tounsi, A., Bousahla, A. A. and Mahmoud, S.R. (2017), "An efficient and simple four variable refined plate theory for buckling analysis of functionally graded plates", *Steel Compos. Struct.*, **25**(3), 257-270. <https://doi.org/10.12989/scs.2017.25.3.257>.
- Benachour A., Hassaine Daouadji T., Ait atman H., Tounsi, A., and Meftah S.A. (2011), "A four variable refined plate theory for free vibrations of functionally graded plates with arbitrary gradient using", *Compos. B Eng.*, **42**(6), 1386-1394. <https://doi.org/10.1016/j.compositesb.2011.05.032>.
- Benchohra, M., Driz, H., Bakora, A., Tounsi, A., Adda Bedia, E. A. and Mahmoud, S.R. (2018), "A new quasi-3D sinusoidal shear deformation theory for functionally graded plates", *Struct. Eng. Mech.*, **65**(1), 19-31. <https://doi.org/10.12989/sem.2018.65.1.019>.
- Benferhat Rabia, Tahar Hassaine Daouadji and Mohamed Said Mansour (2016a), "Free vibration analysis of FG plates resting on the elastic foundation and based on the neutral surface concept using higher order shear deformation theory", *Comptes Rendus Mecanique*, **344**(9), 631-641. <https://doi.org/10.1016/j.crme.2016.03.002>.
- Benferhat Rabia, Tahar Hassaine Daouadji, Lazreg Hadji and Mohamed Said Mansour (2016b), "Static analysis of the FGM plate with porosities", *Steel Compos. Struct.*, **21**(1), 123-136. <https://doi.org/10.12989/scs.2016.21.1.123>.
- Benferhat Rabia, Tahar Hassaine Daouadji, Mohamed Said Mansour and Lazreg Hadji (2016c), "Effect of porosity on the bending and free vibration response of functionally graded plates resting on Winkler-Pasternak foundations", *Eartq. Struct.*, **10**(5), 1429-1449. <https://doi.org/10.12989/eas.2016.10.6.1429>.
- Benferhat, R., Hassaine Daouadji, T. and Mansour, M.S. (2014), "A Higher Order Shear Deformation Model for Bending Analysis of Functionally Graded Plates", *Transactions Indian Institute Metals*, **68**(1), 7-16. <https://doi.org/10.1007/s12666-014-0428-1>.
- Benhenni Mohamed, T. Hassaine Daouadji, Boussad Abbes, Yu Ming LI and Fazilay Abbes (2018), "Analytical and Numerical Results for Free Vibration of Laminated Composites Plates", *J. Chem. Molecul. Eng.*, **12**(6), 300-304.
- Bensattalah Tayeb, Khaled Bouakkaz, Mohamed Zidour and Tahar Hassaine Daouadji (2018), "Critical buckling loads of carbon nanotube embedded in Kerr's medium", *Adv. Nano Res.*, **6**(4), 339-356. <https://doi.org/10.12989/anr.2018.6.4.339>.
- Bouadi, A., Bousahla, A.A., Houari, M.S.A., Heireche, H. and Tounsi, A (2018), "A new nonlocal HSDT for analysis of stability of single layer graphene sheet", *Adv. Nano Res.*, **6**(2), 147-162. <https://doi.org/10.12989/anr.2018.6.2.147>.
- Bouhadra, A., Tounsi, A., Bousahla, A.A., Benyoucef, S. and Mahmoud, S. R. (2018), "Improved HSDT accounting for effect of thickness stretching in advanced composite plates", *Struct. Eng. Mech.*, **66**(1), 61-73. <https://doi.org/10.12989/sem.2018.66.1.061>.
- Carrera, E., Brischetto, S., Cinefra, M. and Soave, M. (2011), "Effects of thickness stretching in functionally graded plates and shells", *Compos. Part B*, **42**, 123-133. <https://doi.org/10.1016/j.compositesb.2010.10.005>.
- Cooke, D.W. and Levinson, M. (1983), "Thick rectangular plates-II, the generalized Lévy solution", *Int. J. Mech. Sci.*, **25**, 207-215. [https://doi.org/10.1016/0020-7403\(83\)90094-2](https://doi.org/10.1016/0020-7403(83)90094-2).
- Demirhan, P.A. and Taskin, V. (2019), "Bending and free vibration analysis of Levy-type porous functionally graded plate using state space approach", *Compos. B Eng.*, **160**, 661-676. <https://doi.org/10.1016/j.compositesb.2018.12.020>.
- El-Haina, F., Bakora, A., Bousahla, A.A., Tounsi, A. and Mahmoud, S.R. (2017), "A simple analytical approach for thermal buckling of thick functionally graded sandwich plates", *Struct. Eng. Mech.*, **63**(5), 585-595. <https://doi.org/10.12989/sem.2017.63.5.585>.
- Fourn, H., Atmane, H.A., Bourada, M., Bousahla, A.A., Tounsi, A. and Mahmoud, S.R. (2018), "A novel four variable refined plate theory for wave propagation in functionally graded material plates", *Steel Compos. Struct.*, **27**(1), 109-122. <https://doi.org/10.12989/scs.2018.27.1.109>.
- Hadji, L. and Adda Bedia, E.A. (2015a), "Influence of the porosities on the free vibration of FGM beams", *Wind Struct.*, **21**(3), 273-287. <https://doi.org/10.12989/was.2015.21.3.273>.
- Hadji, L., Hassaine Daouadji, T. and Adda Bedia, E.A. (2015b), "A refined exponential shear deformation theory for free vibration of FGM beam with porosities", *Geomech. Eng.*, **9**(3), 361-372. <https://doi.org/10.12989/gae.2015.9.3.361>.
- Hassaine Daouadji T. and Belkacem, A., (2017), "Mechanical behaviour of FGM sandwich plates using a quasi-3D higher order shear and normal deformation theory", *Struct. Eng. Mech.*, **61**(1), 49-63. <https://doi.org/10.12989/sem.2017.61.1.049>.
- Hassaine Daouadji T., Belkacem, A., Rabia Benferhat, (2016), "Bending analysis of an imperfect FGM plates under hygro-thermo-mechanical loading with analytical validation", *Adv. Mater. Res.*, **5**(1), 35-53. <https://doi.org/10.12989/amr.2016.5.1.035>.
- Hassaine Daouadji T., Tounsi, A., Adda bedia E.A. (2013), "A New Higher Order Shear Deformation Model for Static Behavior of Functionally Graded Plates", *Appl. Math. Mech.*, **5**(3), 351-364. <https://doi.org/10.1017/S2070073300002721>.
- Hassaine Daouadji, T. (2017), "Analytical and numerical modeling of interfacial stresses in beams bonded with a thin plate", *Adv. Comput. Design*, **2**(1), 57-69. <https://doi.org/10.12989/acd.2017.2.1.057>.
- Hassaine Daouadji, T., Benferhat, R. and Belkacem, A. (2016), "Bending analysis of an imperfect advanced composite plates resting on the elastic foundations", *Coupled Syst. Mech.*, **5**(3), 269-285. <https://doi.org/10.12989/csm.2016.5.3.269>.
- Khalifa, Z., Hadji, L., Hassaine Daouadji, T. and Bourada, M.

- (2018), "Buckling response with stretching effect of carbon nanotube-reinforced composite beams resting on elastic foundation", *Struct. Eng. Mech.*, **67**(2), 125-130. <https://doi.org/10.12989/sem.2018.67.2.125>.
- Lee, K.H., Lim, G.T. and Wang, C.M. (2002), "Thick Lévy plates re-visited", *Int. J. Solids Struct.*, **39**, 127-144. [https://doi.org/10.1016/S0020-7683\(01\)00205-0](https://doi.org/10.1016/S0020-7683(01)00205-0).
- Mantari, J.L., Oktem, A.S. and Guedes Soares, C. (2012) "A new trigonometric shear deformation theory for isotropic, laminated composite and sandwich plates", *Int. J. of Solids and Structures*, **49**, 43-53. <https://doi.org/10.1016/j.ijsolstr.2011.09.008>.
- Menasria, A., Bouhadra, A., Tounsi, A., Bousahla, A. A. and Mahmoud, S. R. (2017), "A new and simple HSDT for thermal stability analysis of FG sandwich plates", *Steel Compos. Struct.*, **25**(2), 157-175. <https://doi.org/10.12989/scs.2017.25.2.157>.
- Mokhtar, Y., Heireche, H., Bousahla, A. A., Houari, M. S. A., Tounsi, A. and Mahmoud, S.R. (2018), "A novel shear deformation theory for buckling analysis of single layer graphene sheet based on nonlocal elasticity theory", *Smart Struct. Syst.*, **21**(4), 397-405. <https://doi.org/10.12989/sss.2018.21.4.397>.
- Rabahi, A., Hassaine Daouadji, T., Benferhat, R. and Adim, B. (2018), "Nonlinear analysis of damaged RC beams strengthened with glass fiber reinforced polymer plate under symmetric loads", *Earthq. Struct.*, **15**(2), 113-122. <https://doi.org/10.12989/eas.2018.15.2.113>.
- Rabia, B., Rabahi, A., Hassaine Daouadji, T., Abbas, B., Adim, B. and Abbas, F. (2018), "Analytical analysis of the interfacial shear stress in RC beams strengthened with prestressed exponentially-varying properties plate", *Adv. Mater. Res.*, **7**(1), 29-44. <https://doi.org/10.12989/amr.2018.7.1.029>.
- Reddy, J.N., Wang, C.M., Lim, G.T. and Ng, K.H. (2001), "Bending solutions of Levinson beams and plates in terms of the classical theories", *J. Solids Struct.*, **38**(2001), 4701-4720. [https://doi.org/10.1016/S0020-7683\(00\)00298-5](https://doi.org/10.1016/S0020-7683(00)00298-5).
- Slimane, M. (2018), "Analysis of bending of ceramic-metal functionally graded plates with porosities using of high order shear theory", *Adv. Eng. Forum*, **30**, 54-70. <https://doi.org/10.4028/www.scientific.net/AEF.30.54>.
- Thai, H.T. and Choi, D.H. (2013), "Finite element formulation of various four unknown shear deformation theories for functionally graded plates", *Finite Elem. Anal. Des.*, **75**(2013), 50-61. <https://doi.org/10.1016/j.finel.2013.07.003>.
- Tounsi, A., Sid Ahmed, H., Benyoucef, S. and Adda Bedia, E.A. (2013), "A refined trigonometric shear deformation theory for thermoelastic bending of functionally graded sandwich plates", *Aerosp. Sci. Technol.*, **24**, 209-220. <https://doi.org/10.1016/j.ast.2011.11.009>.
- Wattanasakulponga, N. and Ungbhakornb, V. (2014), "Linear and non linear vibration analysis of elastically restrained ends FGM beams with porosities", *Aero. Sci. Technol.*, **32**(1), 111-120. <https://doi.org/10.1016/j.ast.2013.12.002>.
- Yazid, M., Heireche, H., Tounsi, A., Bousahla, A. A. and Houari, M. S. A. (2018), "A novel nonlocal refined plate theory for stability response of orthotropic single-layer graphene sheet resting on elastic medium", *Smart Struct. Syst.*, **21**(1), 15-25. <https://doi.org/10.12989/sss.2018.21.1.015>.
- Youcef, D. O., Kaci, A., Benzair, A., Bousahla, A. A. and Tounsi, A. (2018), "Dynamic analysis of nanoscale beams including surface stress effects", *Smart Struct. Syst.*, **21**(1), 65-74. <https://doi.org/10.12989/sss.2018.21.1.065>.
- Younsi, A., Tounsi, A., Zaoui, F. Z., Bousahla, A. A. and Mahmoud, S. R. (2018), "Novel quasi-3D and 2D shear deformation theories for bending and free vibration analysis of FGM plates", *Geomech. Eng.*, **14**(6), 519-532. <https://doi.org/10.12989/gae.2018.14.6.519>.
- Zaoui, F. Z., Ouinas, D. and Tounsi, A. (2019), "New 2D and quasi-3D shear deformation theories for free vibration of functionally graded plates on elastic foundations", *Compos. Part B*, **159**, 231-247. <https://doi.org/10.1016/j.compositesb.2018.09.051>.
- Zenkour, A.M. (2006), "Generalized shear deformation theory for bending analysis of functionally graded plates", *Appl. Math. Modell.*, **30**, 67-84. <https://doi.org/10.1016/j.apm.2005.03.009>.
- Zenkour, A.M. and Radwan, A.F. (2018), "Compressive study of functionally graded plates resting on Winkler-Pasternak foundations under various boundary conditions using hyperbolic shear deformation theory", *Arch. Civil Mech. Eng.*, **18**, 645-658. <https://doi.org/10.1016/j.acme.2017.10.003>.
- Zine, A., Tounsi, A., Draiche, K., Sekkal, M. and Mahmoud, S. R. (2018), "A novel higher-order shear deformation theory for bending and free vibration analysis of isotropic and multilayered plates and shells", *Steel Compos. Struct.*, **26**(2), 125-137. <https://doi.org/10.12989/scs.2018.26.2.125>.
- Zohra A., Lazreg Hadji, Z., Khelifa, T. Hassaine daouadji, E.A. and Adda Bedia (2016), "Analysis of buckling response of functionally graded sandwich plates using a refined shear deformation theory", *Wind Struct.*, **22**(3), 291-305. <https://doi.org/10.12989/was.2016.22.3.291>.

CC